Dysregulation of Amphiregulin stimulates the pathogenesis of cystic lymphangioma

Naofumi Yoshida[a,b,1], Seiji Yamamoto[a,1,2], Takeru Hamashima[a], Noriko Okuno[a], Naruho Okita[a], Shinjiro Horikawa[c], Masao Hayashi[a,d], Thanh Chung Dang[a,e], Quang Linh Nguyen[a], Koichi Nishiyama[f,g], Teruhiko Makino[d], Yoko Ishii[h], Kei Tomihara[b], Tadamichi Shimizu[d], Masabumi Shibuya[i], Makoto Noguchi[b], and Masakiyo Sasahara[a,2]

[a]Department of Pathology, Graduate School of Medicine and Pharmaceutical Sciences, University of Toyama, Toyama 930-0194, Japan; [b]Department of Oral and Maxillofacial Surgery, Graduate School of Medicine and Pharmaceutical Sciences, University of Toyama, Toyama 930-0194, Japan; [c]Intensive Care Unit, Toyama Prefectural Central Hospital, Toyama 930-8550, Japan; [d]Department of Dermatology, Graduate School of Medicine and Pharmaceutical Sciences, University of Toyama, Toyama 930-0194, Japan; [e]Department of Pathophysiology, Vietnam Military Medical University, Hanoi, Vietnam; [f]International Research Center for Medical Sciences, Kumamoto University, 860-0811 Kumamoto, Japan; [g]Department of Medical Sciences, Faculty of Medicine, University of Miyazaki, Miyazaki 889-1601, Japan; [h]Department of Health Science, Faculty of Health and Human Development, The University of Nagano, 380-8525 Nagano, Japan; and [i]Institute of Physiology and Medicine, Jobu University, Gunma 370-1393, Japan

Edited by Napoleone Ferrara, University of California San Diego, La Jolla, CA, and approved April 2, 2021 (received for review September 17, 2020)

Along with blood vessels, lymphatic vessels play an important role in the circulation of body fluid and recruitment of immune cells. Postnatal lymphangiogenesis commonly occurs from preexisting lymphatic vessels by sprouting, which is induced by lymphangiogenic factors such as vascular endothelial growth factor C (VEGF-C). However, the key signals and cell types that stimulate pathological lymphangiogenesis, such as human cystic lymphangioma, are less well known. Here, we found that mouse dermal fibroblasts that infiltrate to sponges subcutaneously implanted express VEGF-D and sushi, Von Willebrand factor type A, EGF, and pentraxin domain containing 1 (SVEP1) in response to PDGFRβ signal. In vitro, *Pdgfrb* knockout (β-KO) fibroblasts had reduced expression of VEGF-D and SVEP1 and overproduced Amphiregulin. Dysregulation of these three factors was involved in the cyst-like and uneven distribution of lymphatic vessels observed in the β-KO mice. Similarly, in human cystic lymphangioma, which is one of the intractable diseases and mostly occurs in childhood, fibroblasts surrounding cystic lymphatics highly expressed Amphiregulin. Moreover, fibroblast-derived Amphiregulin could induce the expression of Amphiregulin in lymphatic endothelial cells. The dual source of Amphiregulin activated EGFR expressed on the lymphatic endothelial cells. This exacerbation cascade induced proliferation of lymphatic endothelial cells to form cystic lymphangioma. Ultimately, excessive Amphiregulin produced by fibroblasts surrounding lymphatics and by lymphatic endothelial cells per se results in pathogenesis of cystic lymphangioma and will be a fascinating therapeutic target of cystic lymphangioma.

cystic lymphangioma | lymphangiogeneis | PDGFRβ CKO | Amphiregulin | pathogenesis

Mammals possess two tightly interconnected vascular systems: the blood vasculature and the lymphatic vasculature. Lymphatic vessels are implicated in the absorption of the interstitial fluid (i.e., the lymph) in all peripheral organs except organs of the nervous system. Lymphangiogenesis, which indicates new growth of the lymphatic vessels, is induced in several pathophysiological conditions such as wound healing. Based on the molecular mechanisms in lymphangiogenesis, wherein physiological lymphangiogenesis requires vascular endothelial growth factor (VEGF)-C (1), pathological lymphangiogenesis is regulated by various growth factors and cytokines such as VEGF-A, -C, -D, fibroblast growth factor 2 (FGF2), hepatocyte growth factor (HGF), insulin-like growth factor 1, and angiopoietin 1 (2, 3) in combination with inflammatory cells such as macrophages (4, 5). However, the mechanism, the type of key signals, and the cell types that are involved in lymphatic vessel formation under pathophysiological conditions in vivo still remain unclear.

The VEGF family and its receptors are essential regulators of both angiogenesis and lymphangiogenesis (6). During new lymphatic vessel formation, it is thought that VEGF-C and VEGF-D can bind to VEGFR3 or VEGFR2, leading to transduction of a proliferation signal (1, 7, 8). While VEGF-C is essential for lymphangiogenesis as a paracrine factor, little is known about the function of VEGF-D, which has been postulated to induce lymphatic vessel formation within tumors, leading to subsequent promotion of metastasis (9).

Regarding the lymphatic vessel remodeling process, recent reports have suggested that sushi, Von Willebrand factor type A, EGF, and pentraxin domain containing 1 (SVEP1), an extracellular matrix protein, is essential for lymphatic remodeling (10, 11). SVEP1 binds integrin α9β1, a cell adhesion receptor involved in lymphangiogenesis, as a high-affinity ligand (12).

Members of the EGF-EGFR system play critical roles in cell proliferation and differentiation in various developmental stages and pathogenesis of many diseases (13). EGFR signaling appeared to positively regulate angiogenesis both directly (14) and indirectly (15). Indeed, EGFR is expressed on human dermal lymphatic endothelial cells in vitro and in vivo, thereby allowing activation of lymphangiogenesis (16).

Significance

Several lymphangiogenic factors, such as vascular endothelial growth factor C (VEGF-C), have been known in normal lymphatics development; however, the key molecules and cell types involved in pathological lymphangiogenesis are less well known. We find that dermal fibroblasts in *Pdgfrb* knockout (β-KO) mice highly express Amphiregulin, and such Amphiregulin causes the cyst-like lymphatic vessels observed in the β-KO mice to form. Similarly, in human cystic lymphangioma, fibroblasts surrounding cystic lymphatics, which highly express Amphiregulin, can also induce the expression of Amphiregulin in lymphatic endothelial cells. Collectively, excessive expression of Amphiregulin results in pathogenesis of cystic lymphangioma. These findings suggest Amphiregulin as a fascinating therapeutic target for patients with cystic lymphangioma.

Author contributions: S.Y. designed research; N.Y., S.Y., T.H., N. Okuno, N. Okita, S.H., M.H., T.C.D., Q.L.N., K.N., T.M., Y.I., and K.T. performed research; S.Y. analyzed data; and S.Y., T.C.D., T.S., M. Shibuya, M.N., and M. Sasahara wrote the paper.

The authors declare no competing interest.

This article is a PNAS Direct Submission.

Published under the PNAS license.

[1]N.Y. and S.Y. contributed equally to this work.

[2]To whom correspondence may be addressed. Email: seiyama@med.u-toyama.ac.jp or sasahara@med.u-toyama.ac.jp.

This article contains supporting information online at https://www.pnas.org/lookup/suppl/doi:10.1073/pnas.2019580118/-/DCSupplemental.

Published May 3, 2021.

Downloaded at Palestinian Territory, occupied on November 27, 2021

www.manaraa.com

Lymphangioma, a form of lymphatic malformation, is considered to be mostly benign and morphologically characterized by small and large thin-walled cysts that occur mainly during childhood (17). Lymphangioma can be sporadically observed anywhere in the body; however, it is particularly common in the head, neck, mediastinum, and axilla (18). Many cases can be treated by sclerotherapy or surgical resection (19, 20). However, severe cases are difficult to treat, and some patients have functional problems such as airway obstruction and cosmetic problems (17, 18). Cellular and molecular mechanisms of the lymphangioma have not yet been fully uncovered.

In this study, we show that PDGFRβ signaling in dermal fibroblasts defines the architecture of hieratical lymphatic vessel structure. We illustrate that dermal fibroblasts express VEGF-D and SVEP1, and that deficiency of the PDGFRβ signal results in reduced production of VEGF-D and SVEP1 in dermal fibroblasts. However, such fibroblasts show overproduction of Amphiregulin, a kind of EGF family ligand. Sponge-implanted PDGFRβ conditional knockout (β-KO) mice exhibit largely dilated and uneven distribution of the formation of lymphatic vessels in vivo. Similarly, in human cystic lymphangioma, the fibroblasts surrounding cystic lymphatics, which highly express Amphiregulin, induced the expression of Amphiregulin in lymphatic endothelial cells. This cascade accelerated proliferation of lymphatic endothelial cells in cystic lymphangioma. These findings suggest that dysregulation of Amphiregulin expression is the cause of pathogenesis of cystic lymphangioma.

Results

Angiogenesis Is Suppressed in the Sponge Matrix of β-KO Mice. Connective tissues growing in the sponge matrices subcutaneously implanted in mice were examined (*SI Appendix*, Figs. S1–S3 and *Supplementary Text*). Newly synthesized connective tissue that had ingrown into the implanted sponge matrix was histologically compared between the two genotypes. The growth end of CD31-positive vessels was traced in CD31 immuno-stained sections (*SI Appendix*, Fig. S4*A*), and the CD31-positive vascularized areas within the sponge matrices were calculated (*SI Appendix*, Fig. S4*B*). The CD31-positive vascularized areas were highly suppressed in the β-KO mice compared to Flox mice of both sexes 14 d after implantation (*SI Appendix*, Fig. S4*B*). Markedly, suppression of the CD31-positive vascularized area was more severe in female mice compared to male mice. To clarify the underlying molecular mechanisms, the expression level of extracellular matrix such as collagens, which are crucially involved in angiogenesis (21), were examined. By real-time PCR analyses, *Col1a1* mRNA was significantly down-regulated in β-KO mice compared to Flox mice (*SI Appendix*, Fig. S4*C*). Moreover, immunohistochemistry of Collagen type I and statistical analysis supported real-time PCR data (*SI Appendix*, Fig. S4 *D* and *E*). In accordance with previous strategies (21), proangiogenic factors were examined. Among the major proangiogenic factors analyzed, including *Vegfa*, *Vegfc*, *Plgf*, *Hgf*, *Fgf2*, and *Cxcl12*, all factors had similar expression levels between the two genotypes. Compared to these, in angiostatic factors, Thrombospondin 1 (TSP1) mRNA, *Thbs1*, was significantly up-regulated in β-KO mice compared to Flox mice (*SI Appendix*, Fig. S4*F*), while other angiostatic factors, such as *Lect1*, *Tnmd*, and *Vash1*, were similar between the two genotypes. In immunohistochemistry, β-KO mice showed increased expression of TSP1 compared to Flox mice (*SI Appendix*, Fig. S4*H*). Statistical analysis of the immuno-positivity of TSP1 staining showed a significant difference between the two genotypes (*SI Appendix*, Fig. S4*G*). It has been shown that TSP1 is degraded through the LRP family of proteins (22). In β-KO mice, while *Lrp1* expression was comparable between the sponges of two genotypes, *Lrp2* (23) expression was greatly decreased (*SI Appendix*, Fig. S5 *A* and *B*). Data from immunofluorescence and intensity analysis showed that the expression of LRP2 protein was significantly suppressed, suggesting that it may be involved in delaying degradation of TSP1 in β-KO mice (*SI Appendix*, Fig. S5 *C* and *D*). In addition, blood vessels of β-KO mice were dilated and partly naked from Neuron-glial antigen 2 (NG2)-positive pericytes (*SI Appendix*, Fig. S6*A*). Statistical analysis of blood-vessel diameter was significantly larger in β-KO mice compared to Flox mice (*SI Appendix*, Fig. S6*B*). These data suggest that PDGFRβ is involved in the growth of blood vessels in the sponge matrix for modulating expression levels of Collagen type I and TSP1 and, in part, is also involved in pericyte dysfunction by suppressing PDGFRβ expression in pericyte on day 14 (*SI Appendix*, Fig. S7).

Highly Disorganized Lymphatic Vessels Are Observed in Sponge Matrix of β-KO Mice. While the CD31-positive vascularized area was larger in female mice than that of male mice on day 14 (*SI Appendix*, Fig. S4*B*), we focused on analyzing specimens from female mice in the later period—on day 28. Intriguingly, the CD31-positive vascularized areas were significantly different; however, the difference seemed relatively small compared to the difference observed on day 14 (Fig. 1*A* and *SI Appendix*, Figs. S4 *A* and *B* and S8*A*). In addition, we found that narrow vasculatures were strongly stained with CD31; large-diameter vasculatures were stained weakly with CD31 (Fig. 1*B*). These immunohistochemistry data prompted us to distinguish whether these CD31-positive vessels in the sponge matrix were blood or lymphatic vessels. To clarify this, we used double staining with lymphatic vessel specific markers LYVE1 or PROX1 in combination with CD31. Immunofluorescence data clearly demonstrated that vessels of a small diameter were CD31-positive but both LYVE1- and PROX1-negative (Fig. 1*C* and *SI Appendix*, Fig. S8*B*). In contrast, vessels that had a relatively large diameter expressed both CD31 and LYVE1 or PROX1 (Fig. 1*C* and *SI Appendix*, Fig. S8*B*), suggesting lymphangiogenesis occurred in this period and that lymphatic vessels may contribute to expansion of vascularized area on day 28.

In the sponge matrixes of day 28, lymphatic vessels were precisely analyzed in Flox and β-KO as well as α-KO, which has been intensively examined in our previous study (21). Intriguingly, the LYVE1-positive lymphatic vessels of β-KO mice were highly dilated and disorganized in shape compared with both Flox and α-KO mice (Fig. 1*D*). This striking lymphatic vessel phenotype was only observed in β-KO mice, suggesting that a PDGFRβ signal and not a PDGFRα signal is intimately implicated in determining the structure of lymphatics. To compare the blood and lymphatic vessels per se in Flox and β-KO, we calculated the actual blood vessel area by subtracting the LYVE1-positive area from the CD31-positive area. We found that the CD31-positive area was comparable between the two genotypes (Fig. 1*E*). In contrast, the actual blood vessel area was smaller in β-KO mice than in Flox mice (Fig. 1*F*). The lymphatic vessel area tended to be larger in β-KO mice, but these results were not statistically significant (Fig. 1*G*). However, both the diameter and distribution of lymphatic vessels were significantly larger and highly uneven in the β-KO mice compared to those in Flox mice (Fig. 1 *H* and *I*).

To dissect the underlying molecular mechanisms behind the differences of lymphatic vessel formation between the two genotypes, we analyzed the expression of lymphangiogenesis-related genes. In real-time PCR analyses of lymphangiogenic VEGFs and VEGFRs using mRNAs extracted from sponge matrixes, *Vegfc* and *Vegfd* mRNAs were significantly suppressed in β-KO mice compared to those in Flox mice (Fig. 2 *B* and *C*), while *Vegfa* mRNA was comparable between the two genotypes (Fig. 2*A*). In major lymphangiogenesis-related receptors, no significant difference was observed in *Flk1*, *Flt4*, or *Nrp2* between Flox mice and β-KO mice (Fig. 2 *D*–*F*). Western blot analysis showed that while VEGF-C protein expression was comparable between the two genotypes (Fig. 2*G*), VEGF-D protein expression was significantly reduced in β-KO mice compared to Flox mice (Fig. 2*H*), which was supported by immunofluorescence data (*SI Appendix*, Fig. S9*A*). It is suggested that VEGF-D is involved in this lymphatic phenotype.

Downloaded at Palestinian Territory, occupied on November 27, 2021

www.manaraa.com

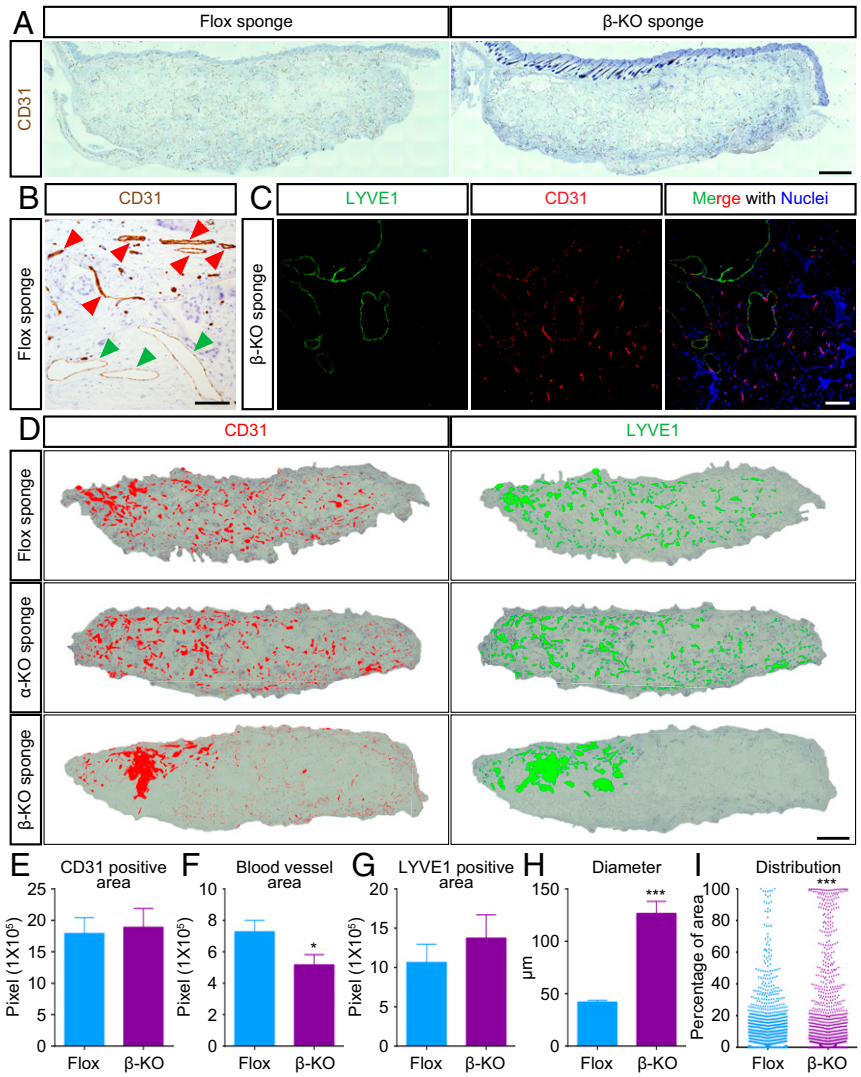

Fig. 1. Formation of lymphatic vessels was cyst-like and uneven in distribution in β-KO mice. (*A*) Immunohistochemistry of CD31 on cross-sectional area of implanted sponges on day 28 after implantation (brown). Sections were counterstained with hematoxylin (pale blue). (*B*) Immunohistochemistry analysis of CD31 is able to visualize both blood vessels (red arrowheads) and lymphatic vessels (green arrowheads). (*C*) Immunofluorescence of LYVE1-positive lymphatic vessels (green) in β-KO sponge costained with CD31 (red). Nuclei are depicted by Hoechst staining (blue). Autofluorescence of sponge is also visualized as blue color. (*D*) Immunohistochemistry of CD31 and LYVE1 on cross-sectional area of implanted sponges of Flox, α-KO, and β-KO on day 28 after implantation. CD31-positive and LYVE1-positive vessel areas and the lumen areas surrounded by both CD31-positive and LYVE1-positive vessels are filled by pseudocolor red and green, respectively. (*E–I*) Cyst-like lymphatic vessels were exclusively observed in β-KO mice. Measured and calculated CD31-positive area (*E*), blood vessel area (*F*), and LYVE1-positive lymphatic vessel area (*G*) (n = 9 to 11 mice per group). (*H* and *I*) Lymphatic vessels of β-KO show highly dilated (*H*) and uneven distribution (*I*) (n = 4 mice per group). *P < 0.05 versus Flox mice; ***P < 0.001 versus Flox mice [Scale bars: 1 mm (*A* and *D*) and 100 μm (*B* and *C*).]

Moreover, recently reported SVEP1 (10, 11), which is critically involved in appropriate lymphatic vessel remodeling, was measured by real-time PCR. *Svep1* mRNA was significantly reduced in β-KO mice compared to Flox mice (Fig. 2*I*). In immunohistochemistry, while SVEP1 was expressed in the sponge matrix of Flox mice, weaker immuno-positivity of SVEP1 was observed in β-KO mice (Fig. 2*J*), which was reconfirmed by immunofluorescence data (*SI Appendix*, Fig. S9*B*). Statistical analysis showed that the immunoreactivity was significantly reduced in β-KO mice compared to Flox mice (Fig. 2*K*). In a receptor for SVEP1, integrin α9β1 (12), no significant differences were observed in such *Itga9* and *Itgb1* mRNAs between both genotypes.

β-KO Fibroblasts Play Crucial Roles in Appropriate Lymphatic Vessel Formation. Since fibroblasts are the major cellular component in the sponge matrix and are responsible for abundant expression of PDGFRβ (*SI Appendix*, Figs. S1 *E* and *F* and S3*A*), fibroblasts must be analyzed for the primary source of VEGF-D and SVEP1. By using in vitro dermal fibroblasts (21, 24), mRNA expression of such genes was measured by real-time PCR. *Vegfd* mRNA was significantly down-regulated in β-KO fibroblasts compared to Flox fibroblasts (Fig. 2*L*). In immunocytochemistry, β-KO fibroblasts expressed a low level of VEGF-D compared to Flox fibroblasts (Fig. 2*M*). Statistical analysis of the immunoreactivity of VEGF-D showed significant differences between the two genotypes (Fig. 2*N*). *Svep1* mRNA was also significantly down-regulated in β-KO fibroblasts compared to Flox fibroblasts (Fig. 2*O*). Immunocytochemistry and statistical analysis of SVEP1 data supported the real-time PCR data (Fig. 2 *P* and *Q*). Previous scientific studies have suggested that both VEGF-D and SVEP1 knockout mice exhibited hypomorphic and dysfunctional lymphatic vasculature (11, 25). These findings may suggest that PDGFRβ

Downloaded at Palestinian Territory, occupied on November 27, 2021

www.manaraa.com

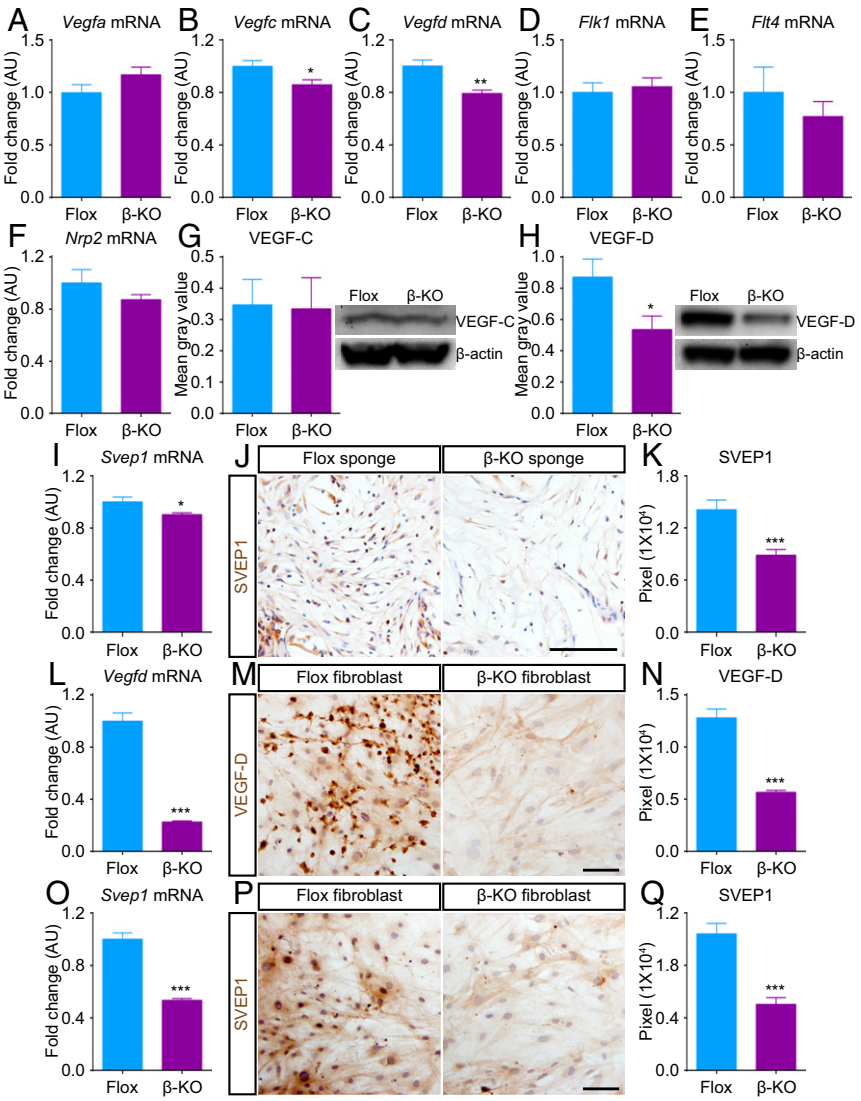

Fig. 2. Molecular mechanisms underlying the formation of cyst-like lymphatic vessels in implanted sponges of β-KO mice. (*A–F*) Lymphangiogenic ligands and receptors of VEGF family are measured by real-time PCR using mRNAs from sponges. *Vegfa* mRNA (*A*) is comparable in both genotypes, but both *Vegfc* (*B*) and *Vegfd* (*C*) mRNAs are significantly down-regulated in sponge of β-KO mice. The receptors for these ligands, *Flk1* (*D*), *Flt4* (*E*), and *Nrp2* (*F*) mRNAs, are similar level in both genotypes ($n = 5$ to 7 mice per group). (*G* and *H*) Western blotting data of VEGF-C (*G*) and VEGF-D (*H*). Whereas VEGF-C protein shows comparable level between two genotypes (*G*), VEGF-D protein is significantly reduced in β-KO sponge (*H*) ($n = 6$ mice per group). (*I–K*) *Svep1* mRNA is significantly down-regulated in β-KO sponge (*I*). Immunohistochemistry supports the real-time PCR data (*J*), and statistical analysis of immunohistochemistry shows significantly the difference between two genotypes (*K*). Sections were counterstained with hematoxylin (pale blue) ($n = 5$ to 7 mice per group). (*L–N*) VEGF-D is reduced in β-KO fibroblasts in vitro. *Vegfd* mRNA is significantly down-regulated in β-KO fibroblasts compared with that of Flox fibroblasts (*L*). Immunocytochemistry of VEGF-D (brown) supports real-time PCR data (*M*), and statistical analysis shows significant difference between both genotypes (*N*). (*O–Q*) SVEP1 is reduced in β-KO fibroblasts in vitro. *Svep1* mRNA is significantly down-regulated in β-KO fibroblasts compared with that of Flox fibroblasts (*O*). Immunocytochemistry of SVEP1 (brown) supports real-time PCR data (*P*), and statistical analysis shows significant difference between both genotypes (*Q*) ($n =$ 7 samples per group in real-time PCR, $n = 6$ samples per group in immunocytochemistry). $*P < 0.05$ versus Flox mice; $**P < 0.01$ versus Flox mice; $***P < 0.001$ versus Flox mice or fibroblasts. [Scale bars: 100 μm (*J*, *M*, and *P*).]

signaling of dermal fibroblasts, at least in part, defines appropriate lymphatic vessel structure and distribution through production of VEGF-D and SVEP1.

The EGFR Signal Is Involved in the Formation of Cyst-Like Lymphatic Vessels in β-KO. It has been reported that both VEGF-D and SVEP1 knockout mice show hypomorphic and dysfunctional lymphatic vasculature (11, 25). To explore the underlying molecular mechanisms of cyst-like expansion of lymphatic vessels observed in β-KO sponges, we conducted in vitro culture experiments using fibroblasts, which are derived from both Flox and β-KO mice and human skin lymphatic endothelial cells (HMVECdLy). Firstly, HMVECdLy were stimulated in supplemented conditioned medium (CM) from Flox or β-KO (*SI Appendix*, Fig. S10*A*); specimens of HMVECdLy were incubated for 20 min with CM before they were subsequently used for phospho-kinase arrays (*SI Appendix*, Fig. S10 *B* and *C*) and real-time PCR (*SI Appendix*, Fig. S10 *D–I*). Slight but certain differences could be observed in phospho-ERK1/2 between Flox and β-KO (*SI Appendix*, Fig. S10 *B* and *C*), and mRNA expression of cell cycle indicators *CCNA1, CCNB1, CCND3*, and *CCNE1* was highly up-regulated (*SI Appendix*, Fig. S10 *D–G*). Moreover, cell cycle inhibitor *CDKN1A* (p21 mRNA)

Downloaded at Palestinian Territory, occupied on November 27, 2021

www.manaraa.com

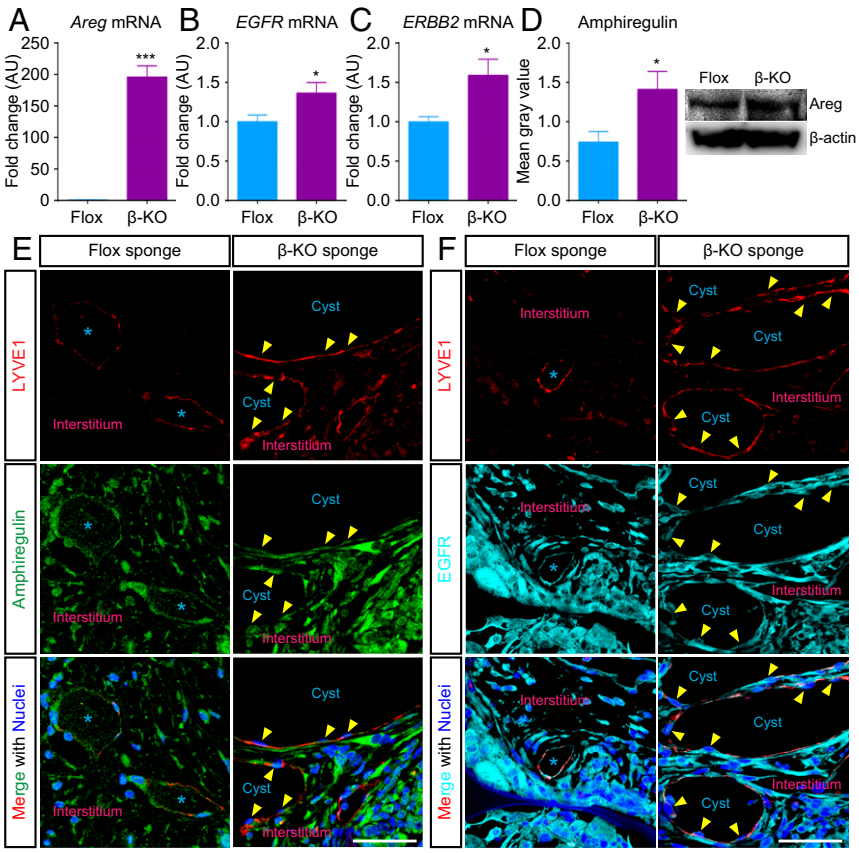

Fig. 3. β-KO fibroblasts exhibit overproduction of Amphiregulin and stimulate proliferation of lymphatic endothelial cells via EGFR. (*A*) mRNA of Amphiregulin, an EGFR ligand, was drastically induced in β-KO fibroblasts in coculture model in vitro (*SI Appendix*, Fig. S11*A*). (*B* and *C*) mRNAs of EGFR (*B*) and ERBB2 (*C*) were significantly induced in HMVECdLy in coculture model in vitro (*SI Appendix*, Fig. S11*A*) ($n = 6$ samples per group). (*D*) Amphiregulin protein expression level was significantly higher in sponges of β-KO mice than those of Flox mice as confirmed by Western blotting ($n = 6$ mice per group). $^*P < 0.05$ versus Flox fibroblast group or mice; $^{***}P < 0.001$ versus Flox fibroblasts. (*E* and *F*) Multicolor immunofluorescence of Flox and β-KO sponges. LYVE1 (red) and Amphiregulin (green) in *E*, LYVE1 (red) and EGFR (cyan) in *F*. Asterisks in Flox sponges indicate lumen of lymphatic vessels. Arrowheads in β-KO sponges indicate lymphatic endothelial cells. Nuclei were depicted by Hoechst (blue). [Scale bars: 50 μm (*E* and *F*).]

was down-regulated, and proliferation marker *PCNA* was significantly up-regulated (*SI Appendix*, Fig. S10 *H* and *I*). These data suggest that CM from β-KO fibroblasts could accelerate proliferation in HMVECdLy via the ERK1/2 signal pathway.

Next, to identify the ligand(s) and receptor(s) that are involved in HMVECdLy proliferation, Transwell cocultures were conducted (*SI Appendix*, Fig. S11*A*). HMVECdLy that were cocultured for 3 d with Flox or β-KO fibroblasts were used for phospho-kinase arrays (*SI Appendix*, Fig. S11 *B* and *C*). Again, certain differences could be observed in phospho-ERK1/2 and phospho-EGFR between Flox and β-KO (*SI Appendix*, Fig. S11 *B* and *C*). To investigate which EGF family ligands were involved, mRNA expression levels of the ligands were confirmed. Whereas many mRNAs of the ligands were decreased in β-KO fibroblasts cocultured with HMVECdLy (*SI Appendix*, Fig. S12 *A*–*J*), *Areg* (Fig. 3*A*), *Hbegf*, and *Nrg4* (*SI Appendix*, Fig. S12 *E* and *I*) were up-regulated. However, whereas *Hbegf* was significantly up-regulated in β-KO fibroblasts, single culture of both Flox and β-KO was comparable to the expression of *Hbegf* mRNA (*SI Appendix*, Fig. S13). Regarding *Nrg4* expression, Neuregulin 4 can bind to ERBB4 (*SI Appendix*, Fig. S12 *K* and *L*) but not EGFR (26). These data suggest that Amphiregulin should be the candidate ligand, and both HBEGF and Neuregulin 4 were excluded as a candidate. EGFR and ERBB2, which are receptors for Amphiregulin, were significantly up-regulated in HMVECdLy cocultured with β-KO fibroblasts compared with those of Flox fibroblasts (*SI Appendix*, Fig. S11*A* and Fig. 3 *B* and *C*). Moreover, Amphiregulin protein expression was significantly higher in β-KO sponges on day 14 than in Flox mice (Fig. 3*D*). In immunofluorescence, Amphiregulin abundantly expressed mainly in fibroblasts in the vicinity of cyst-like lymphatic vessels in β-KO mice, whereas a small number of fibroblasts in interstitium expressed Amphiregulin in Flox mice (Fig. 3*E*). LYVE1-positive lymphatic endothelial cells expressed EGFR in both genotypes as confirmed by immunofluorescence study (Fig. 3*F*). Collective data suggest that Amphiregulin, in coordination with VEGF-D and SVEP1, plays an important role in the formation of cyst-like lymphatic vessels in β-KO sponges (*SI Appendix*, Fig. S14).

Amphiregulin-Expressing Fibroblasts May Be Involved in the Formation of Cystic Lymphangioma in Humans. To confirm whether Amphiregulin-expressing fibroblasts contribute to the progression of human cystic lymphangioma, skin biopsy samples were examined. A typical adult cystic lymphangioma lesion was clinically observed on the upper arm of the patient (Fig. 4*A*). Highly swollen lumen can be observed in the Hematoxylin and Eosin (H&E) staining section of the biopsy sample to be confirmed as the lesion of cystic lymphangioma (Fig. 4*A*). In immunofluorescence, Amphiregulin mainly expressed fibroblasts in the vicinity of lymphatic vessels of the specimens of cystic lymphangioma, but was not abundant in control specimens (Fig. 4*B*). In the pixel-based morphometrical analysis of the biopsy samples (*SI Appendix*, Fig. S15*A*), Amphiregulin expression in the specimens of cystic lymphangioma was significantly higher than that of the control

Downloaded at Palestinian Territory, occupied on November 27, 2021

www.manaraa.com

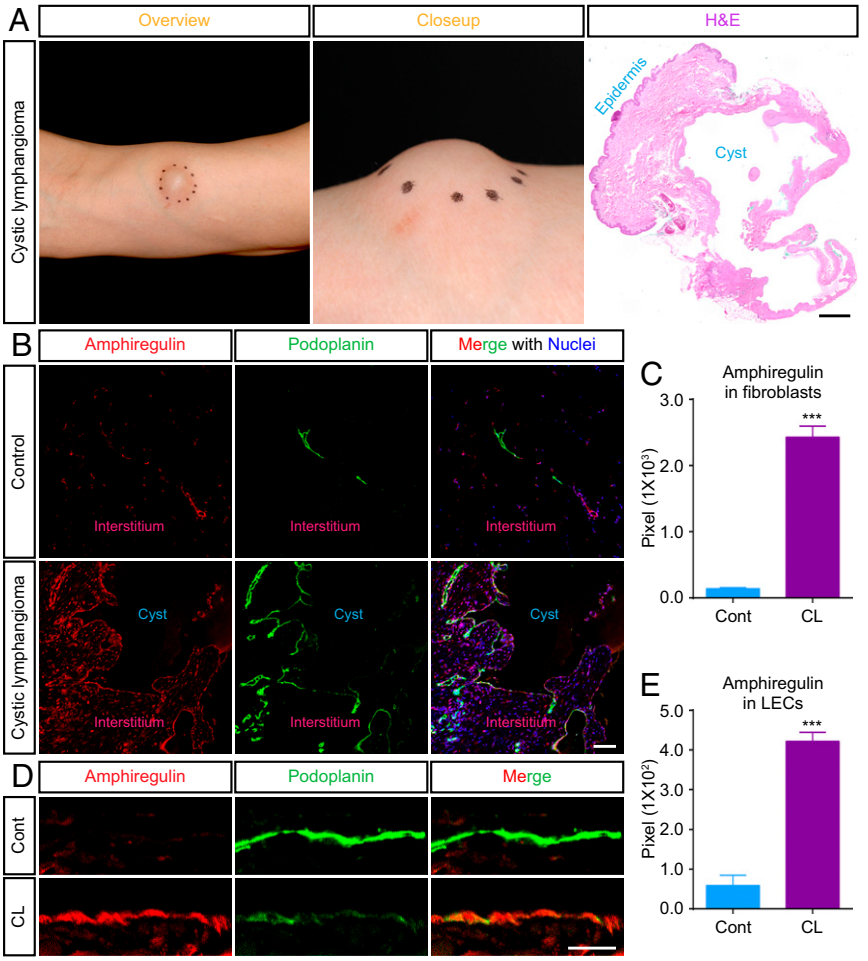

Fig. 4. Amphiregulin expressed in the fibroblasts in the vicinity of lymphatic vessels in human cystic lymphangioma. (*A*) Overview (*Left*) and closeup (*Middle*) of the lesion of cystic lymphangioma was clinically observed on the upper arm of the adult patient. The Hematoxylin and Eosin (H&E) staining section of the biopsy sample from the same patient shows a large cyst under the skin, which is the hallmark of the cystic lymphangioma (*Right*). (*B* and *C*) Amphiregulin is highly expressed in the fibroblasts of patients with cystic lymphangioma. Immunofluorescence of Amphiregulin (red) was observed in fibroblasts in the vicinity of Podoplanin-positive lymphatic vessels (green) in the specimens of cystic lymphangioma, whereas Amphiregulin-positive fibroblasts were few in the specimen from controls (*B*). Nuclei were depicted by Hoechst (blue). Statistical analysis data of Amphiregulin intensity show significantly the difference between control (Cont) and cystic lymphangioma (CL) (*C*) [$n = 48$ areas (50 μm × 50 μm) randomly chosen from 3 patients each (16 areas from 1 patient)]. (*D* and *E*) Amphiregulin is also highly expressed in the lymphatic endothelial cells of the patient with cystic lymphangioma. Immunofluorescence of Amphiregulin (red) was unquestionably observed in the lymphatic endothelial cells, which are weak positive with Podoplanin immunostaining (green), in the specimen of CL, whereas Amphiregulin expression level in lymphatic endothelial cells was under the detection level in the specimen from Cont (*D*). Statistical analysis data of Amphiregulin intensity in lymphatic endothelial cells (LECs) show significantly the difference between Cont and CL (*E*) [$n = 30$ areas (50 μm × 16.7 μm) randomly chosen from 3 specimens each (10 areas from 1 patient)]. ***$P < 0.001$ versus control [Scale bars: 1 mm (*A*, *Right*), 100 μm (*B*), and 20 μm. (*D*)]

specimens (Fig. 4*C*). Precise observation found that lymphatic endothelial cells of cystic lymphangioma unquestionably expressed Amphiregulin, while little or no Amphiregulin was expressed in control specimens (Fig. 4*D*). Significant differences in Amphiregulin expression levels on lymphatic endothelial cells could be observed between the two groups of the biopsy samples (Fig. 4*E*). Supporting these data, lymphatic endothelial cells in β-KO sponges also expressed Amphiregulin (Fig. 3*E*), and HMVECdLy cocultured with β-KO fibroblasts significantly up-regulated *AREG* mRNA (*SI Appendix*, Fig. S15 *B–E*). In addition, Podoplanin expression levels of lymphatic endothelial cells in specimens from cystic lymphangioma, which are the adluminal areas protruding toward the center of the cyst, were significantly lower than those in the controls (Fig. 5 *A* and *B*). The coculture model results (*SI Appendix*, Fig. S15*C*) also suggested that low-level expression of Podoplanin may be supportive evidence of lymphatic endothelial cell proliferation and lymphatic dilation as reported by a previous study (9). Finally, we confirmed that EGFR signaling was highly increased in lymphatic endothelial cells in the specimens from patients with cystic lymphangioma (Fig. 5*C*), and these findings are summarized in Fig. 5*D*.

Inhibition of Amphiregulin Alleviates Cyst-Like Lymphatic Vessels in β-KO Sponges. To confirm whether the cyst-like lymphatic vessels are alleviated by inhibition of Amphiregulin, we conducted a treatment experiment using anti-Amphiregulin neutralizing antibody (Ab) and Erlotinib, which can inhibit EGFR activation by Amphiregulin. The Erlotinib-treated group showed alleviated cyst-like lymphatic vessels (Fig. 6*A*), and the diameter of lymphatics was significantly smaller than that of β-KO mice (Fig. 6*B*). Intriguingly, highly suppressed lymphatic vessel formation was observed in the anti-Amphiregulin Ab treated group compared to β-KO mice (Fig. 6 *A* and *B*). In addition, the result of Student's *t* test between the Erlotinib-treated group and the anti-Amphiregulin Ab–treated group was statistically significant

Downloaded at Palestinian Territory, occupied on November 27, 2021

www.manaraa.com

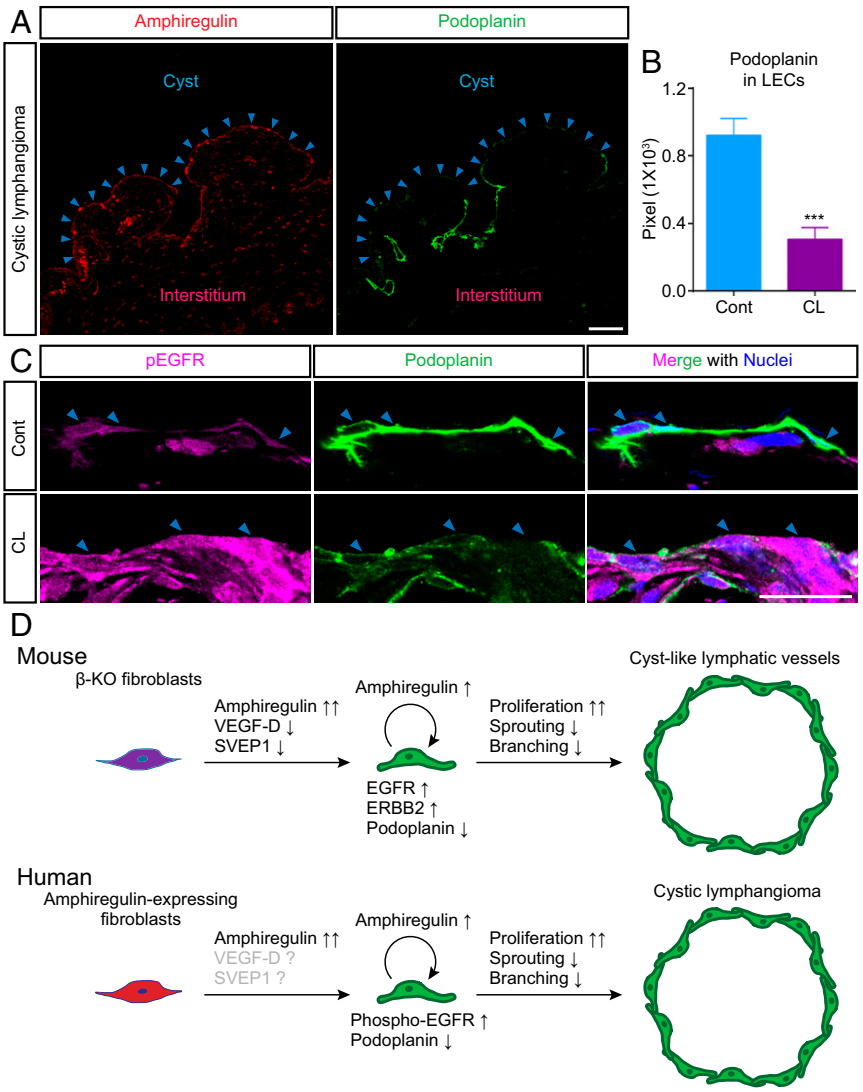

Fig. 5. Amphiregulin derived from fibroblasts modulates the status of lymphatic endothelial cells in vivo. (*A* and *B*) Podoplanin appeared to be down-regulated in lymphatic endothelial cells in the specimen of cystic lymphangioma. In the specimen from cystic lymphangioma, Podoplanin (green) expression level was down-regulated in the lymphatic endothelial cells (arrowheads), which also highly express Amphiregulin (red) (Fig. 4 *D* and *E*), judged by immunofluorescence (*A*). Statistical analysis of Podoplanin intensity in LECs showed significantly difference between Cont and CL (*B*) [$n = 30$ areas (50 μm × 16.7 μm) randomly chosen from 3 patients each (10 areas from 1 patient)]. ***$P < 0.001$ versus control. (*C*) Phospho-EGFR (pEGFR) signal (magenta) was highly detected in the lymphatic endothelial cells (green, arrowheads) in the specimens from patients with cystic lymphangioma [Scale bars: 100 μm (*A*) and 20 μm (*C*).] (*D*) Proposed molecular cascades of Amphiregulin-induced cystic lymphatic vessel formation in the β-KO mice and patients with cystic lymphangioma.

($P < 0.001$). This suggests that anti-Amphiregulin Ab treatment may be more effective than Erlotinib treatment for ameliorating cyst-like lymphatic vessels observed in β-KO mice.

Discussion

The PDGF-PDGFR system plays crucial roles in tissue remodeling in wound healing processes such as granulation formation, angiogenesis, and lymphangiogenesis (21, 27). The present study is a characterization of the specific functional contributions of PDGFRβ in connective tissue remodeling processes such as angiogenesis and lymphangiogenesis using the sponge implantation model (*SI Appendix*, *Supplementary Discussion*).

It has been reported that VEGF-D–deficient mice show hypomorphic dermal lymphatics (25), and that SVEP1-deficient mice exhibit significantly smaller-sized lymphatic vessels due to the remodeling perturbation (10, 11). The phenotype of highly dilated cyst-like lymphatics observed in β-KO mice did not resemble the hypomorphic lymphatics that are observed in VEGF-D– and SVEP1-deficient mice. It suggests that the cyst-like lymphatic vessels did not merely depend on the reduced expression levels of VEGF-D and SVEP1.

So far, the mice deleting *Pdgfb* gene in lymphatic endothelial cells exhibited dilated lymphatics caused by suppression of smooth muscle cell (SMC) recruitment (28). However, in the case of β-KO mice, it was uncovered that Amphiregulin expressed in β-KO fibroblasts, not perturbation of SMC recruitment to lymphatic vessels, centrally acts to accelerate proliferation of lymphatic endothelial cells. We concluded that β-KO fibroblasts induced the expression of Amphiregulin and decreased the expression of VEGF-D and SVEP1 in the vicinity of lymphatic vessels in sponges. Such excess Amphiregulin accelerated proliferation of lymphatic endothelial cells, and low level of VEGF-D and SVEP1 might contribute to suppress the lymphatic sprouting and branching. Eventually, dilated cyst-like lymphatic vessels were formed in β-KO mice.

Downloaded at Palestinian Territory, occupied on November 27, 2021

www.manaraa.com

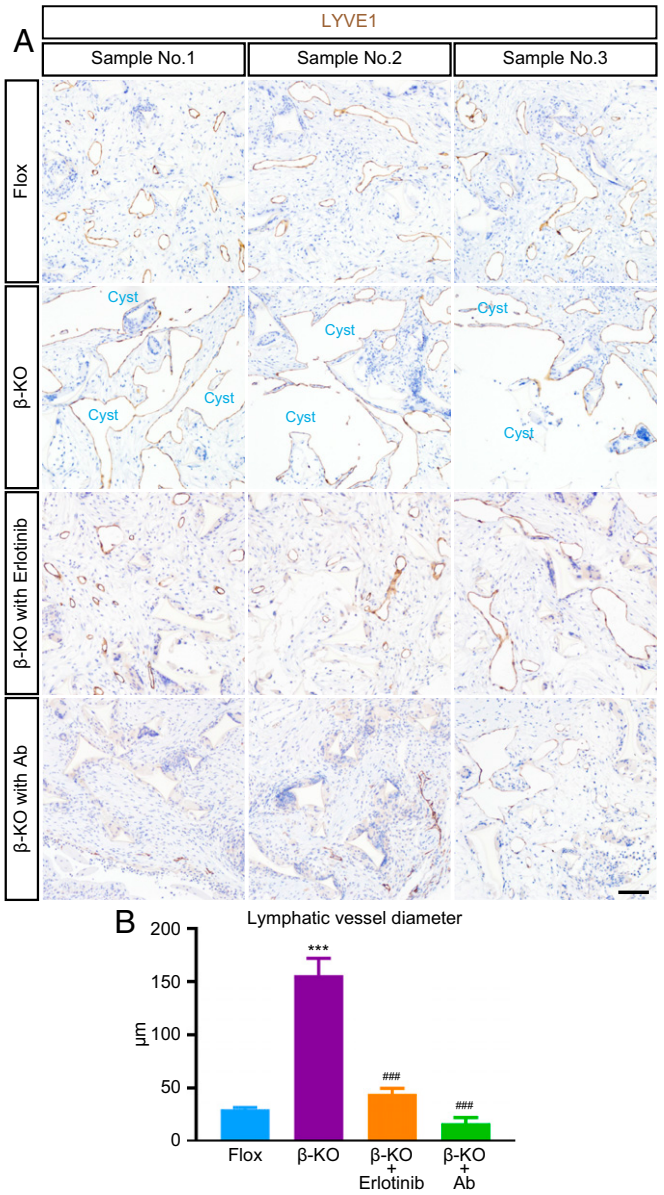

Fig. 6. Treatment experiment of β-KO mice using neutralizing antibody and inhibitor. (*A*) Immunohistochemical evaluation of the treatment effect of anti-Amphiregulin neutralizing antibody (Ab) and Erlotinib, an inhibitor of EGFR signal. Representative three different sponge sections from three different individuals in each group were shown. Highly swollen cyst-like lymphatic vessels (brown) were observed in β-KO mice compared to Flox mice, Erlotinib treated β-KO mice, and anti-Amphiregulin Ab treated β-KO mice, all of which exhibit small-sized lymphatic vessels. Nuclei were depicted by hematoxylin (pale blue). (Scale bar: 100 μm.) (*B*) Statistical analysis data of lymphatic vessel diameter ($n = 3$ to 4 mice). ***$P < 0.001$ versus Flox. ###, $P < 0.001$ versus β-KO.

Human cystic lymphangioma has been morphologically characterized as small and large thin-walled cysts that occur mainly in children (17) and sometimes in adults, and it is commonly observed in the head, neck, mediastinum, and axilla (18); however, it is sporadically found anywhere in the human body. Several genes have been linked to cystic lymphangioma (29), but underlying cellular and molecular mechanisms still remain unclear. Our findings using the specimens from human cystic lymphangioma strongly suggested that the fibroblasts surrounding cystic lymphatics, which highly express Amphiregulin, induced the expression of Amphiregulin in lymphatic endothelial cells. This cascade accelerated proliferation of lymphatic endothelial cells to form lymphatic cysts in cystic lymphangioma.

In conclusion, using a sponge-implantation mouse model, we have shown that PDGFRβ mediates connective tissue remodeling. Angiogenesis is interdependent and is a crucial component of connective tissue remodeling. We demonstrated that the reduction of collagen deposition, which is similar to data of α-KO mice (21), and excessive TSP1 production by *Pdgfrb*-inactivated mice is likely to be the main reason for the substantial delay of angiogenesis in the β-KO mice (*SI Appendix*, Fig. S7), which is the different mechanism of suppression of angiogenesis compared to α-KO mice. In the lymphangiogenesis in β-KO mice, VEGF-D and SVEP1, both of which may be involved in normal lymphatic vessel formation, were reduced in β-KO mice and β-KO fibroblasts. In addition, Amphiregulin, which is an accelerator of cell proliferation, was highly induced in β-KO mice in vivo and β-KO fibroblasts in vitro. Dysregulation of these three factors in β-KO mice exhibited the formation of cyst-like lymphatic vessels (*SI Appendix*, Fig. S14). Our findings demonstrate that the PDGFRβ signal of dermal fibroblasts defines the architecture of lymphatic vessel structure in mice. Although the precise underlying mechanisms linking between PDGFRβ signal and the expression of VEGF-D, SVEP1, and Amphiregulin remain to be determined in a future study, this study opens an avenue to the understanding of the role of PDGFRβ signal in lymphangiogenesis.

In mice and humans, Amphiregulin-expressing fibroblasts in the vicinity of lymphatic vessels might contribute to inducing lymphatic endothelial cell hyperproliferation to form lesions of cystic lymphangioma (Fig. 5*D*). Treatment experiments using the anti-Amphiregulin Ab and Erlotinib demonstrated therapeutic effects against cyst-like lymphatic vessels of β-KO mice, and the efficiency of anti-Amphiregulin Ab was greater than that of Erlotinib. In the clinical setting, our findings strongly suggest that Amphiregulin is considered to be a therapeutic target for the patients of cystic lymphangioma.

Materials and Methods

Ethics. All animal procedures were conducted in accordance with guidelines laid out by the Institutional Animal Care and Use Committee at the University of Toyama (University of Toyama, Sugitani, Toyama City, Japan). All study protocols were approved by the Ethics Committee of the University of Toyama. The use of human samples was approved by the Ethics Committee of the University of Toyama, and samples were handled in accordance with the Declaration of Helsinki. Informed consent was obtained from the patients in an appropriate manner.

Animals. Descriptive analyses were performed on the following transgenic mouse lines: *CAGGCre-ER*$^{+/-}$;*Pdgfrb*$^{flox/flox}$ (β-KO mouse) (30–32), *Pdgfrb*$^{flox/flox}$ (Flox mouse), and *CAGGCre-ER*$^{+/-}$;*Pdgfra*$^{flox/flox}$ (α-KO mouse) (21, 33, 34).

Sponge Implantation and Suppression of PDGFRβ Expression. Sponge implantation was performed as previously described (21). On days 14 and 28 after implantation, connective tissue–formed sponges were excised together with the enclosed sponge implants under deep anesthesia. The obtained tissues were used for real-time PCR, Western blotting, and histological studies. See *SI Appendix, Supplementary Materials and Methods* for remaining methods.

Immunohistochemistry and Immunofluorescence Staining. The specimens were incubated at 4 °C overnight for one or two nights with the primary antibodies. Colorimetric immunostaining was done using the appropriate Histofine Simple Stain Mice System (Nichirei Biosciences Inc.) and 3,3′-diaminobenzidine tetrahydrochloride (DAB, Dako) reaction. For immunofluorescence, fluorescent dye–conjugated secondary antibodies (Thermo Fisher Scientific) were used at 4 °C overnight. See *SI Appendix, Supplementary Materials and Methods* for remaining methods.

Western Blotting. Sample preparations and all other procedures for Western blotting have been described elsewhere (32, 35). Briefly, tissue lysates were separated by SDS-PAGE and then electrophoretically transferred to

Downloaded at Palestinian Territory, occupied on November 27, 2021
www.manaraa.com

polyvinylidene difluoride membranes. The membranes were then probed with the primary antibodies at 4 °C overnight. The membranes were incubated with the appropriate secondary antibodies. Immunoreactive bands were detected using enhanced chemiluminescence reagents (GE Healthcare Bio-Sciences AB) according to the manufacturer's instructions. See *SI Appendix, Supplementary Materials and Methods* for remaining methods.

Cell Culture. Cell culture was performed as previously described (21, 24, 34). Briefly, fibroblasts prepared from *Pdgfrb*$^{flox/flox}$;*Cre-ER*$^{TM+/-}$, *Pdgfrb*$^{flox/flox}$;*Cre-ER*$^{TM-/-}$ pups were subjected with 1 μM of 4-hydroxytamoxifen (4-OHT, Sigma-Aldrich) for deleting of Floxed allele for 48 h in order to obtain β-KO and control Flox fibroblasts, respectively. Coculture using fibroblasts and HMVECdLy (Lonza) were conducted according to manufacturer's instructions (Corning Incorporated). See *SI Appendix, Supplementary Materials and Methods* for remaining methods.

Real-Time PCR. Real-time PCR was performed as previously reported (32, 33, 36). Briefly, cDNAs were diluted 1:25 in the reaction mixture containing SYBR Premix EX Taq II (Takara Bio Inc.). Real-time PCR was performed with a Takara Thermal Cycler Dice Real Time System TP800 (Takara Bio Inc.). For data analysis, the mouse *beta-actin* (*Actb*) housekeeping genes were used as an internal control. Induction values were calculated using analysis software (Takara Bio Inc.). See *SI Appendix, Supplementary Materials and Methods* for remaining methods.

Phospho-Kinase Array. The comprehensive phospho-kinase analyses were performed using the Human Phospho-Kinase array kit (R&D Systems) according to the manufacturer's instructions. Briefly, lysates of HMVECdLy were used after centrifuge to remove the cell debris. The phospho-kinase array membranes were incubated with the cell lysates. After being washed with wash buffer, membranes were developed by the reagents included in the kit (R&D Systems). The intensity of each spot was analyzed by the ImageJ software (NIH) and compared with the negative- and positive-control spots.

Treatment Experiment. Sponge-implanted β-KO mice were administered anti-mouse Amphiregulin neutralizing antibody (R&D Systems) or Erlotinib (Selleck Chemicals). Mice were given 5 μg neutralizing antibody in 200 μL PBS or 50 mg/kg Erlotinib in dimethyl sulfoxide 3 times a week. See *SI Appendix, Supplementary Materials and Methods* for remaining methods.

Statistical Analysis. Comparisons between two experimental groups were made using unpaired Student's *t* tests. Multivariate analyses were made with one-way analysis of variance followed by Turkey's analyses. *P* values less than 0.05 were considered statistically significant. Graphs were created using GraphPad Prism 9 (GraphPad Software, Inc.). Quantified data are presented as mean ± SEM.

Data Availability. All study data are included in the article and/or *SI Appendix*.

ACKNOWLEDGMENTS. We thank members of the Department of Pathology and Life Science Research Center, University of Toyama for their thoughtful discussions and careful animal care, and we also thank Professor Kari Alitalo, with whom we had valuable discussion and who provided suggestions, and Professor Masataka Majima, who taught us the animal model during a previous project. This work was supported by Grant-in-Aid for Scientific Research (JP24659112 to S.Y., JP25293093 and JP17H04062 to M. Sasahara) and Scientific Research on Innovative Areas (JP23122506 to S.Y.) from The Ministry of Education, Culture, Sports, Science and Technology. This work was also supported by the Translational Research program, Strategic PRomotion for Practical Application of INnovative Medical Technology (A119 to S.Y.) from the Japan Agency for Medical Research and Development.

1. M. J. Karkkainen *et al*., Vascular endothelial growth factor C is required for sprouting of the first lymphatic vessels from embryonic veins. *Nat. Immunol.* **5**, 74–80 (2004).
2. T. Tammela, K. Alitalo, Lymphangiogenesis: Molecular mechanisms and future promise. *Cell* **140**, 460–476 (2010).
3. T. Watabe, Roles of transcriptional network during the formation of lymphatic vessels. *J. Biochem.* **152**, 213–220 (2012).
4. D. Kerjaschki, The crucial role of macrophages in lymphangiogenesis. *J. Clin. Invest.* **115**, 2316–2319 (2005).
5. S. F. Schoppmann *et al*., Tumor-associated macrophages express lymphatic endothelial growth factors and are related to peritumoral lymphangiogenesis. *Am. J. Pathol.* **161**, 947–956 (2002).
6. H. Takahashi, M. Shibuya, The vascular endothelial growth factor (VEGF)/VEGF receptor system and its role under physiological and pathological conditions. *Clin. Sci. (Lond.)* **109**, 227–241 (2005).
7. M. G. Achen *et al*., Vascular endothelial growth factor D (VEGF-D) is a ligand for the tyrosine kinases VEGF receptor 2 (Flk1) and VEGF receptor 3 (Flt4). *Proc. Natl. Acad. Sci. U.S.A.* **95**, 548–553 (1998).
8. V. Joukov *et al*., A novel vascular endothelial growth factor, VEGF-C, is a ligand for the Flt4 (VEGFR-3) and KDR (VEGFR-2) receptor tyrosine kinases. *EMBO J.* **15**, 290–298 (1996).
9. V. Schacht *et al*., T1alpha/podoplanin deficiency disrupts normal lymphatic vasculature formation and causes lymphedema. *EMBO J.* **22**, 3546–3556 (2003).
10. T. Karpanen *et al*., An evolutionarily conserved role for Polydom/Svep1 during lymphatic vessel formation. *Circ. Res.* **120**, 1263–1275 (2017).
11. N. Morooka *et al*., Polydom is an extracellular matrix protein involved in lymphatic vessel remodeling. *Circ. Res.* **120**, 1276–1288 (2017).
12. R. Sato-Nishiuchi *et al*., Polydom/SVEP1 is a ligand for integrin α9β1. *J. Biol. Chem.* **287**, 25615–25630 (2012).
13. D. J. Riese, 2nd, D. F. Stern, Specificity within the EGF family/ErbB receptor family signaling network. *BioEssays* **20**, 41–48 (1998).
14. C. H. Baker *et al*., Blockade of epidermal growth factor receptor signaling on tumor cells and tumor-associated endothelial cells for therapy of human carcinomas. *Am. J. Pathol.* **161**, 929–938 (2002).
15. R. Kumar, R. Yarmand-Bagheri, The role of HER2 in angiogenesis. *Semin. Oncol.* **28**, 27–32 (2001).
16. D. Marino *et al*., Activation of the epidermal growth factor receptor promotes lymphangiogenesis in the skin. *J. Dermatol. Sci.* **71**, 184–194 (2013).
17. C. Damaskos *et al*., Cystic hygroma of the neck: Single center experience and literature review. *Eur. Rev. Med. Pharmacol. Sci.* **21**, 4918–4923 (2017).
18. A. Gedikbasi *et al*., Multidisciplinary approach in cystic hygroma: Prenatal diagnosis, outcome, and postnatal follow up. *Pediatr. Int.* **51**, 670–677 (2009).
19. L. Jiao-Ling *et al*., Treatment and prognosis of fetal lymphangioma. *Eur. J. Obstet. Gynecol. Reprod. Biol.* **231**, 274–279 (2018).
20. S. L. Woolley, D. R. Smith, S. Quine, Adult cystic hygroma: Successful use of OK-432 (picibanil). *J. Laryngol. Otol.* **122**, 1260–1264 (2008).
21. S. Horikawa *et al*., PDGFRα plays a crucial role in connective tissue remodeling. *Sci. Rep.* **5**, 17948 (2015).
22. I. Mikhailenko, M. Z. Kounnas, D. K. Strickland, Low density lipoprotein receptor-related protein/alpha 2-macroglobulin receptor mediates the cellular internalization and degradation of thrombospondin. A process facilitated by cell-surface proteoglycans. *J. Biol. Chem.* **270**, 9543–9549 (1995).
23. C. Spuch, S. Ortolano, C. Navarro, LRP-1 and LRP-2 receptors function in the membrane neuron. Trafficking mechanisms and proteolytic processing in Alzheimer's disease. *Front. Physiol.* **3**, 269 (2012).
24. Z. Gao *et al*., Deletion of the PDGFR-beta gene affects key fibroblast functions important for wound healing. *J. Biol. Chem.* **280**, 9375–9389 (2005).
25. S. Paquet-Fifield *et al*., Vascular endothelial growth factor-d modulates caliber and function of initial lymphatics in the dermis. *J. Invest. Dermatol.* **133**, 2074–2084 (2013).
26. A. Gumà, V. Martínez-Redondo, I. López-Soldado, C. Cantó, A. Zorzano, Emerging role of neuregulin as a modulator of muscle metabolism. *Am. J. Physiol. Endocrinol. Metab.* **298**, E742–E750 (2010).
27. Y. Ishii, T. Hamashima, S. Yamamoto, M. Sasahara, Pathogenetic significance and possibility as a therapeutic target of platelet derived growth factor. *Pathol. Int.* **67**, 235–246 (2017).
28. Y. Wang *et al*., Smooth muscle cell recruitment to lymphatic vessels requires PDGFB and impacts vessel size but not identity. *Development* **144**, 3590–3601 (2017).
29. V. L. Luks *et al*., Lymphatic and other vascular malformative/overgrowth disorders are caused by somatic mutations in PIK3CA. *J. Pediatr.* **166**, 1048–1054.e1-5 (2015).
30. Y. Ishii *et al*., Mouse brains deficient in neuronal PDGF receptor-beta develop normally but are vulnerable to injury. *J. Neurochem.* **98**, 588–600 (2006).
31. H. Kitahara *et al*., The novel pathogenesis of retinopathy mediated by multiple RTK signals is uncovered in newly developed mouse model. *EBioMedicine* **31**, 190–201 (2018).
32. H. Sato *et al*., PDGFR-β plays a key role in the ectopic migration of neuroblasts in cerebral stroke. *Stem Cells* **34**, 685–698 (2016).
33. T. C. Đặng *et al*., Powerful homeostatic control of oligodendroglial lineage by PDGFRα in adult brain. *Cell Rep.* **27**, 1073–1089.e5 (2019).
34. K. Yamada *et al*., Different PDGF receptor dimers drive distinct migration modes of the mouse skin fibroblast. *Cell. Physiol. Biochem.* **51**, 1461–1479 (2018).
35. S. Yamamoto *et al*., Essential role of Shp2-binding sites on FRS2alpha for corticogenesis and for FGF2-dependent proliferation of neural progenitor cells. *Proc. Natl. Acad. Sci. U.S.A.* **102**, 15983–15988 (2005).
36. S. Yamamoto *et al*., Inflammation-induced endothelial cell-derived extracellular vesicles modulate the cellular status of pericytes. *Sci. Rep.* **5**, 8505 (2015).

Downloaded at Palestinian Territory, occupied on November 27, 2021

www.manaraa.com